IEEE TRANSACTIONS ON

POWER ELECTRONICS

A PUBLICATION OF THE IEEE POWER ELECTRONICS SOCIETY

This Print Collection Contains the Following Issues:

JULY	2009	VOLUME 24	NUMBER 7	ITPEE8	(ISSN 0885-8993)
AUGUST	2009	VOLUME 24	NUMBER 8		

For the July 2009 issue, see p. 1669 for the Table of Contents.
For the August 2009 issue, see p. 1857 for the Table of Contents.

IEEE

Celebrating 125 Years
of Engineering the Future

IEEE TRANSACTIONS ON

POWER ELECTRONICS

A PUBLICATION OF THE IEEE POWER ELECTRONICS SOCIETY

AUGUST 2009 VOLUME 24 NUMBER 8 ITPEE8 (ISSN 0885-8993)

(Contents Continued on Page 1858)

Celebrating 125 Years
of Engineering the Future

(Contents Continued from Page 1857)

INFORMATION FOR AUTHORS

IEEE TRANSACTIONS ON POWER ELECTRONICS (ISSN 0885-8993) is published bimonthly in print and monthly online by The Institute of Electrical and Electronics Engineers, Inc. Responsibility for the contents rests upon the authors and not upon the IEEE, the Society/Council, or its members. **IEEE Corporate Office**: 3 Park Avenue, 17th Floor, New York, NY 10016-5997. **IEEE Operations Center**: 445 Hoes Lane, Piscataway, NJ 08854-4141. **NJ Telephone**: +1 732 981 0060. **Price/Publication Information**: Individual copies: IEEE Members $20.00 (first copy only), nonmembers $258.00 per copy. (Note: Postage and handling charge not included.) Member and nonmember subscription prices available upon request. Available in microfiche and microfilm. Periodicals Postage Paid at New York, NY, and at additional mailing offices. **Postmaster**: Send address changes to "IEEE TRANSACTIONS ON POWER ELECTRONICS, IEEE, 445 Hoes Lane, Piscataway, NJ 08854-4141. GST Registration No. 12564188. Printed in U.S.A."

Anisotropy Comparison of Reluctance and PM Synchronous Machines for Position Sensorless Control Using HF Carrier Injection

Hugo W. De Kock, *Member, IEEE*, Maarten J. Kamper, *Senior Member, IEEE*, and Ralph M. Kennel, *Senior Member, IEEE*

***Abstract*—Position sensorless control of reluctance and permanent magnet synchronous machines at zero and low speed is possible using HF voltage injection and proper demodulation. The so-called saliency position, which is tracked by the HF sensorless scheme, is different from the actual rotor position: the difference contains both offset and rotor-position-varying components, which may be explained by carefully considering the HF behavior of the machine and the effect that fundamental excitation and rotor position have upon it. This paper gives insight into the HF behavior of synchronous machines and serves as a practical guide for implementation of stable and robust position estimation at zero and low speed.**

***Index Terms*—AC machines, electrical engineering, estimation.**

I. Introduction

THE FOCUS on high-efficiency and cost-effective drives for applications ranging from washing machines to electrical cars has led to the adoption of certain types of synchronous machines, with control algorithms that avoid the use of expensive sensors, as well as maximize their efficiency. Permanent magnet synchronous machines (PMSMs) are widely accepted due to their high torque to volume ratio. Especially, those that exhibit rotor saliency characteristics, since they are prime candidates for position sensorless control, even at zero speed [1]–[22]. The reluctance synchronous machine (RSM) represents an alternative to the PMSM for some applications, and the construction cost could be cheaper due to the lack of PMs. The RSM is known for its rotor saliency characteristics and is therefore definitely a candidate for sensorless control [23]–[41]. The introduction of concentrated stator windings, instead of distributed stator windings, represents another cost-saving effort. The implications on the fundamental control, as well as sensorless control, have to be considered [14], [42], [43].

To have field-orientated torque control in the entire speed range, rotor position estimation in the entire range is necessary. At high speed (and a reasonable amount of total flux linkage magnitude), a back-EMF observer may be used to find the rotor position. At low speed, the lack of back-EMF nessesitates an alternative position estimation scheme to be used, namely, one that relies on rotor saliency. Ultimately, a combination of methods is necessary to have an accurate rotor position estimation in the entire speed range [16], [38], [44].

One method of position estimation at low and zero speed applies a continuous alternating HF voltage with the inverter, and digitally processess the resulting HF currents to obtain a saliency-dependent position, which may be called the anisotropy position or the saliency position [8], [22], [41]. When there is hardly any rotor saliency, e.g., the surface-mounted PMSM or the induction machine, it is difficult to track such a saliency position. In some machines like the RSM, PM-assisted RSM, and interior PMSM, the inherent rotor saliency property enables rotor position detection at zero speed [18], [19].

It may be the case that there exist multiple saliencies (or a saliency with multiple harmonics) [2], [22], in which case special care has to be taken to track a useful one. In the case of a single dominant saliency that rotates in the same direction as the rotor and at the electrical speed, the anisotropy position (saliency position) may be equal to the actual rotor position. However, the fundamental frequency excitation (torque producing current and flux linkage) may have a great impact upon the saliency position: saturation may reduce the effective saliency (reducing SNR in the HF current signal) and cross saturation may cause the saliency position to deviate from the actual rotor position (offset error) [14], [16], [22], [38], [40], [41]. Nonsinusoidal flux distribution, i.e., position-dependent inductances in the synchronous reference frame that are caused by, e.g., stator slot openings or concentrated windings, also has an impact on the saliency position so that it deviates from the actual rotor position (rotor-position-dependent error) [41].

In this paper, the effective HF model for a transverse-laminated RSM with normal distributed windings is presented based on practical tests on an experimental setup. It is shown how the saliency position deviates from the actual rotor position under load (offset error) and during rotation (rotor-position-dependent error). A simple load-dependent compensation function is suggested to compensate the offset error [41]. The experiment is then also repeated for a commercially available PMSM. The difference in HF behavior is pointed out. This paper gives insight into the HF behavior of synchronous machines and serves

Manuscript received November 20, 2008; revised January 21, 2009. Current version published August 12, 2009. Recommended for publication by Associate Editor J. O. Ojo.

H. W. De Kock was with the Department of Electrical and Electronic Engineering, Stellenbosch University, Matieland 7602, South Africa. He is now with the Development Department, Optimal Energy, Cape Town 8001, South Africa (e-mail: hugodekock@gmail.com).

M. J. Kamper is with the Department of Electrical and Electronic Engineering, Stellenbosch University, Matieland 7602, South Africa (e-mail: kamper@sun.ac.za).

R. M. Kennel is with the Elektrische Antriebssysteme und Leistungselektronik, Fakultät EI, Technische Universität München, München 80333, Germany (e-mail: kennel@ieee.org).

Digital Object Identifier 10.1109/TPEL.2009.2017537

as a practical guide to implement a robust and stable position estimation at low and zero speed.

II. Machine Model

Neglecting the end winding and core losses, the voltage space vector equation for both RSM and PMSM is given in the stationary $\alpha\beta$ reference frame by (1). The flux linkage vector $\vec{\psi}_s$ is a nonlinear function of the magnetizing current vector $\vec{i}_s$ and has, in theory, a sinusoidal distribution in space, i.e., with respect to the electrical rotor position θ_r. The flux linkage vector $\vec{\psi}_s$ is the total flux linkage, i.e., it includes the leakage flux linkage. The transformation to the synchronously rotating dq reference frame, as in (2), should remove the dependency of the flux linkage vector on θ_r, so that $\vec{\psi}_r$ is only a function of $\vec{i}_r$. However, in reality, the flux linkage distribution is not perfectly sinusoidal, due to, e.g., stator slot openings or concentrated windings. Therefore, $\vec{\psi}_r$ remains a function of θ_r. As mentioned, $\vec{\psi}_r$ is a nonlinear function of $\vec{i}_r$, since in any machine design there is a certain amount of saturation and cross coupling.

The relationship between the flux linkage and the current may be expressed in terms of inductance, and it can be understood in matrix notation as in (4): there are self-inductance terms on the diagonal and mutual inductance (also called coupling inductance) terms on the off-diagonal, where it should be clear that these are differential (also called tangential) inductances, i.e., partial derivatives. Ideally L_d and L_q would be constant, and L_{dq} as well as $\frac{\partial \vec{\psi}_r}{\partial \theta_r}$ would be zero. However, due to the nonlinear properties of machines, these inductances are again nonlinear functions of $\vec{i}_r$ and θ_r, and there are flux pulsations with movement, i.e., $\frac{\partial \vec{\psi}_r}{\partial \theta_r}$ is not zero

$$\vec{u}_s = R \cdot \vec{i}_s + \frac{d\vec{\psi}_s}{dt} \tag{1}$$

$$\vec{u}_r = \vec{u}_s \cdot e^{-j\theta_r} \tag{2}$$

$$= R \cdot \vec{i}_r + \frac{d\vec{\psi}_r}{dt} + j \cdot \omega_r \cdot \vec{\psi}_r \tag{3}$$

$$\omega_r = \frac{d\theta_r}{dt}$$

$$\begin{bmatrix} \frac{d\psi_d}{dt} \\ \frac{d\psi_q}{dt} \end{bmatrix} = \begin{bmatrix} L_d & L_{dq} \\ L_{dq} & L_q \end{bmatrix} \begin{bmatrix} \frac{di_d}{dt} \\ \frac{di_q}{dt} \end{bmatrix} + \begin{bmatrix} \frac{\partial \psi_d}{\partial \theta_r} \\ \frac{\partial \psi_q}{\partial \theta_r} \end{bmatrix} \frac{d\theta_r}{dt}. \tag{4}$$

For an HF model of the machine, consider (3) while applying an HF voltage vector: the resistive loss term and the speed voltage term become insignificant to the derivative of the flux linkage term, as expressed in (5). This equation can further be approximated as (6) if ω_r is sufficiently smaller than ω_{HF}

$$\vec{u}_r(\omega_{\mathrm{HF}}) \approx \frac{d\vec{\psi}_r}{dt} \tag{5}$$

$$\begin{bmatrix} u_d \\ u_q \end{bmatrix} \approx \begin{bmatrix} L_d & L_{dq} \\ L_{dq} & L_q \end{bmatrix} \begin{bmatrix} \frac{di_d}{dt} \\ \frac{di_q}{dt} \end{bmatrix}. \tag{6}$$

III. Position Sensorless Control

Assuming a perfect anisotropy (saliency), i.e., constant L_d and L_q, with $L_d \neq L_q$ and $L_{dq} = 0$, a pulsating HF voltage vector can be superimposed on the fundamental control voltage vector, then the resulting HF current vector can be filtered out from the measured current. The saliency position information that is found within the HF current allows one to estimate the saliency position. From the estimated saliency position, the rotor position may be estimated, as described by numerous authors including those of [8], [41], and [22]. Of course, we would like to use the inherent rotor saliency that is provided by the physical rotor design [18], [19], so that the saliency position closely resembles the rotor position. So that we do not get confused between the fundamental frequency model and the anisotropy model, we use the subscript A and describe the ideal anisotropy as constant L_{dA} and L_{qA} with $L_{dA} \neq L_{qA}$ and $L_{dqA} = 0$.

The estimation process is described mathematically, in easy-to-follow and logical steps, by (7)–(26) and is illustrated by the block diagrams in Figs. 2 and 3. The saliency position estimation takes place within a reference frame that is aligned with the anisotropy (saliency). A pulsating HF voltage is applied in an arbitrary direction δ, as in (8), with respect to the estimated saliency position $\hat{\theta}_A$. The common choices are $\delta = 0$ or $\delta = \frac{\pi}{2}$, although it has been suggested that the injection direction should resemble the maximum torque per ampere (MTPA) axis in an effort to minimize the effect of inductance change due to saturation [20].

The HF voltage amplitude U_{HF} is usually chosen as constant and needs to be large enough to give a substantial HF current. If the machine has a very small inductance, then a small voltage amplitude causes a relatively large HF current. It has been suggested that the voltage amplitude be varied in an effort to reduce acoustic noise [21], so that it only has a high value during acceleration or high load.

The chosen frequency ω_{HF} also largely influences the amplitude of the HF current and the acoustic noise, and needs to be selected so that digital filters can successfully separate the HF current from the fundamental frequency current so that the current vector controller does not influence the HF currents much, i.e., a certain amount of frequency separation is needed. In many papers and also in our experience $\omega_{\mathrm{HF}} = 2\pi \cdot 500$ [rad/s] was a good choice for the machines at hand.

Following the definitions (7) and (8), the alternating HF voltage in stationary reference frame is given by (9), and so the alternating voltage in the reference frame aligned to the actual anisotropy at position θ_A is given by (10). This alternating voltage causes the HF current in the actual anisotropy reference frame as in (11). The current angle of $\vec{i}_A$ is given by ϕ_A. It should be noted that if $L_{dA} = L_{qA}$, this current angle simplifies to $\phi_A = -\tilde{\theta}_A$. Assuming a slowly varying error $\tilde{\theta}_A$, the HF current in the actual anisotropy reference frame may be approximated as in (12). However, since we do not know θ_A and only have access to $\hat{\theta}_A$, we need to find the expression for the HF current in the estimated anisotropy reference frame, as in (14). The useful information, i.e., the modulated amplitude of $\vec{i}_{\hat{A}}$, is expressed by (15)

$$\vec{u}_{\mathrm{HF}} = U_{\mathrm{HF}} \cos(\omega_{\mathrm{HF}} t) + j0 \tag{7}$$

$$\vec{u}_{\hat{A}} = \vec{u}_{\mathrm{HF}} e^{j\delta} \tag{8}$$

$$\vec{u}_{s\mathrm{HF}} = \vec{u}_{\hat{A}} e^{j\hat{\theta}_A} \tag{9}$$

$$\vec{u}_A = \vec{u}_{s\mathrm{HF}} \cdot e^{-j\theta_A} = \vec{u}_{\hat{A}} e^{-j\tilde{\theta}_A} \tag{10}$$

$$\tilde{\theta}_A = \theta_A - \hat{\theta}_A$$

$$\begin{bmatrix} i_{dA} \\ i_{qA} \end{bmatrix} = \begin{bmatrix} L_{dA} & 0 \\ 0 & L_{qA} \end{bmatrix}^{-1} \begin{bmatrix} \int u_{dA}\, dt \\ \int u_{qA}\, dt \end{bmatrix} \tag{11}$$

$$\vec{i}_A \approx \vec{\psi}_{\mathrm{HF}} \left(\frac{1}{L_{dA}} \cos\tilde{\theta}_A - j \frac{1}{L_{qA}} \sin\tilde{\theta}_A \right) \tag{12}$$

$$\vec{\psi}_{\mathrm{HF}} = \frac{U_{\mathrm{HF}}}{\omega_{\mathrm{HF}}} \sin(\omega_{\mathrm{HF}} t + \zeta) e^{j\delta}$$

$$\phi_A = \mathrm{atan} \left(\frac{-L_{dA} \sin\tilde{\theta}_A}{L_{qA} \cos\tilde{\theta}_A} \right) \tag{13}$$

$$\vec{i}_{\hat{A}} = \vec{i}_A e^{j\tilde{\theta}_A} = \vec{\psi}_{\mathrm{HF}} \cdot \vec{A} \tag{14}$$

$$\vec{A} = \left(\frac{1}{\Sigma L} + \frac{1}{\Delta L} e^{j2\tilde{\theta}_A} \right) \tag{15}$$

$$\Sigma L = 2 \frac{L_{qA} \cdot L_{dA}}{L_{qA} + L_{dA}}$$

$$\Delta L = 2 \frac{L_{qA} \cdot L_{dA}}{L_{qA} - L_{dA}}.$$

To facilitate understanding, (7)–(15) are illustrated by two vector diagrams in Fig. 1(a) and (b). To simplify the diagrams, the voltage injection angle δ is chosen as zero so that $\vec{u}_{\hat{A}} = \vec{u}_{\mathrm{HF}}$. Note that all vectors in this diagram are alternating (not rotating); therefore, the diagram represents only a snapshot in time where both $\cos(\omega_{\mathrm{HF}} t) > 0$ and $\sin(\omega_{\mathrm{HF}} t) > 0$. It is worth noting that the imaginary part of $\vec{i}_{\hat{A}}$ is zero when either $\tilde{\theta}_A = 0$ or $L_{dA} = L_{qA}$: this means it is zero when the estimated anisotropy reference frame is aligned with the actual anisotropy reference frame, or when no anisotropy exists. Assuming that the anisotropy does exist, it is, therefore, possible to find the anisotropy position by driving the imaginary part of $\vec{i}_{\hat{A}}$ to zero.

The superposition of the HF voltage vector onto the fundamental control voltage vector, as in (16) and Fig. 2, results in an HF current vector that can be separated from the fundamental frequency current vector with a bandpass filter (BPF), as in (17). We are only interested in the useful information given by $\vec{A}$ and can get this from $\vec{i}_{\hat{A}}$ using the demodulation given in (18). The demodulation sine wave F_{dem}, as in (19), has the phase shift ζ, which should be zero in theory. In practice the phase shift between HF voltage and HF current could be larger than 90° due to digital system delays. In the demodulation, it is, therefore, important to check that the HF current and the demodulation sine wave F_{dem} are in phase by setting ζ to an appropriate value.

Now, using the imaginary part of $\vec{A}$, as in (20), as the input signal to a PI controller, i.e. driving this signal to zero, we can assume that $\tilde{\theta}_A$ will be small and (21) becomes valid. Therefore,

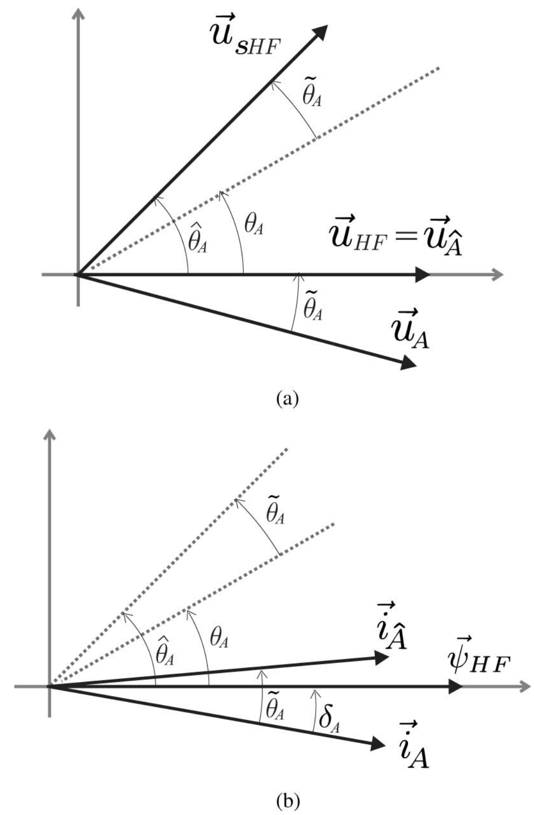

Fig. 1. Vector diagrams illustrating HF signal amplitudes. (a) Applied HF voltage. (b) HF current response.

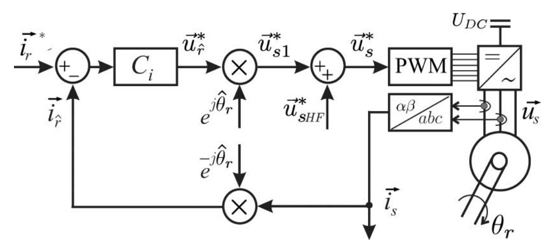

Fig. 2. Fundamental current control.

in this closed-loop tracking system [see (22)–(24)], or phase-locked loop (PLL), we can be sure to track the saliency position, and the speed at which it moves, wherever it may be. Important is the normalization with the constant ΔL in (20) and the sign that it has, since negative feedback (stability) has to be ensured.

As the final step, we may estimate the rotor position θ_r from our estimated saliency position $\hat{\theta}_A$ as in (25), and in the ideal case, θ_{comp} is zero or a constant. We can also estimate the rotor speed using our estimated anisotropy speed, as in (26). Since $\hat{\omega}_A$ is used, in part, to drive the integrator so that the saliency position is tracked, and therefore, might have large and fast changes, we might need additional low-pass filtering to obtain a reasonable rotor speed estimation

$$\vec{u}_s^* = \vec{u}_{s1}^* + \vec{u}_{s\mathrm{HF}} \tag{16}$$

$$\vec{i}_{\hat{A}} = \mathrm{BPF}\left\{ \vec{i}_s e^{-j\hat{\theta}_A} \right\} \tag{17}$$

$$\vec{A} = \text{LPF}\left\{\vec{i}_{\hat{A}} e^{-j\delta} \cdot F_{\text{dem}}\right\} \tag{18}$$

$$F_{\text{dem}} = 2\frac{\omega_{\text{HF}}}{U_{\text{HF}}}\sin(\omega_{\text{HF}}t + \zeta) \tag{19}$$

$$\sin(2\tilde{\theta}_A) = (\Delta L)\,\Im m\left\{\vec{A}\right\} \tag{20}$$

$$2\tilde{\theta}_A \approx \sin(2\tilde{\theta}_A) \tag{21}$$

$$\tilde{\theta}_A = \theta_A - \hat{\theta}_A \tag{22}$$

$$\hat{\omega}_A = K_i \int \tilde{\theta}_A\, dt \tag{23}$$

$$\hat{\theta}_A = \int \left(K_p\tilde{\theta}_A + \hat{\omega}_A\right) dt \tag{24}$$

$$\hat{\theta}_r = \hat{\theta}_A + \theta_{\text{comp}} \tag{25}$$

$$\hat{\omega}_r = \text{LPF}\left\{\hat{\omega}_A\right\}. \tag{26}$$

IV. Reluctance Synchronous Machine

A laboratory 1.5 kW RSM, with a rated current of 3.5 A rms and a rated torque of 10 N·m was used to test the sensorless field-oriented control scheme for zero and low speed as described earlier.

The first test is to find a suitable HF voltage vector. A rotating voltage vector is applied for frequencies ranging from 0 to 1000 Hz, and current vector response is inspected. At low frequencies, the current amplitude is large, the phase difference between the voltage vector and the current vector is small, and the rotor might turn. When increasing the frequency, the current magnitude reduces and the phase shift between the voltage and the current increases. At high frequencies, a sound can be heard, which could be rather unpleasant. Although the theoretical limit for the phase shift between the voltage and the current vector is 90°, a phase shift that is greater than 90° is measured, which is explained by the digital system delay. For this RSM, a voltage vector (rotating or alternating) with a frequency of 508 Hz and an amplitude of 100 V (this represents 30% of the total available voltage using space vector PWM and a dc bus voltage of 580 V), results in an HF current vector that has a phase delay of 113° with respect to the voltage vector and an amplitude of 400 mA (about 10% of the rated current). The sound that the high-frequency signals produce is barely noticeable. Therefore, $\zeta = 113° - 90° = 23°$ in (19), so that the demodulation sine wave will be in phase with our HF current response. Since the sampling frequency is $f_s = 12,205$ Hz and the HF waveform has a frequency of 508 Hz, this phase shift of 23° only means about two samples delay.

The second test is to get an idea of the parameter values L_{dA} and L_{qA} at no load. It is assumed that the saliency position θ_A is equal to the rotor position θ_r. The rotor position θ_r is kept at zero and the estimated saliency position $\hat{\theta}_A$ is varied from 2π to zero, i.e., the error $\theta_r - \hat{\theta}_A$ varies from zero to 2π. The HF voltage is applied, as shown in Fig. 3, and the signal $\vec{A}$ is inspected. It is observed that the frequency component $2\omega_{\text{HF}}$ is visible in $\vec{A}$ and that its suppression depends on the cutoff frequency and order of the low-pass filter (LPF). A second-order LPF that gives us 40 dB suppression at $2\omega_{\text{HF}}$ is chosen. From the real part of $\vec{A}$, i.e., the real part in (15), there is enough information to calculate L_{dA} and L_{qA}. When using the measured values of $\Re e\{\vec{A}\}$ for a complete cycle of $\hat{\theta}_A = 2\pi..0$, the calculation gives $L_{dA} = 0.33976$ H and $L_{qA} = 0.26488$ H. By using these values to normalize $\vec{A}$ and to subtract the offset from the real part of $\vec{A}$, the signal $e^{j2\tilde{\theta}}$ becomes visible. Fig. 4 shows this measurement, where the top graph is $\tilde{\theta}_A$, the middle graph is $\vec{A}$, and the bottom graph is the normalized $\vec{A}$ with the offset subtracted from the real part.

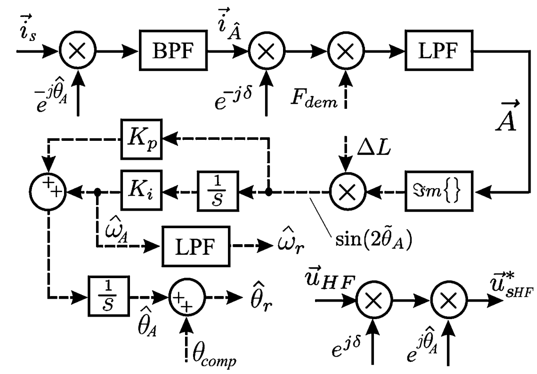

Fig. 3. Rotor position estimation.

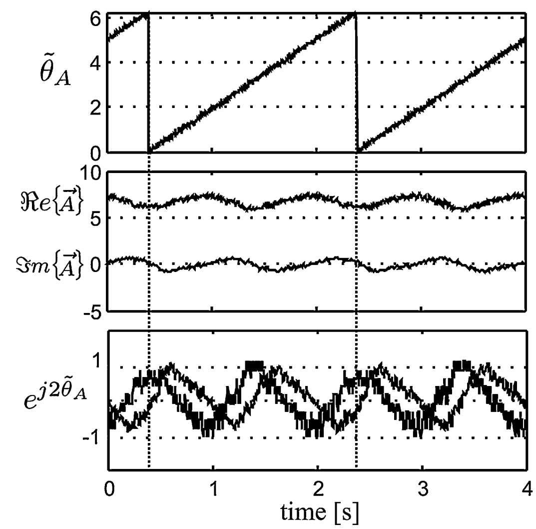

Fig. 4. RSM anisotropy at no load and standstill.

It has previously been shown in [41] that for this RSM, the anisotropy parameters, or HF inductances, L_{dA} and L_{qA} are load-dependent, and that there is a certain amount of mutual inductance. In general, increasing the load also increases the amount of saturation, which reduces the inductance. This result is shown here again in Fig. 5. Note that the fundamental frequency current is applied at a constant current angle of 60°, which is an approximation to maximum torque per ampere (MTPA) for this RSM.

When the closed-loop position estimation is active, there is a load-dependent offset error between the estimated saliency position and the actual rotor position due to the mutual inductance [22], [38], [40], [41]. There might be some stability

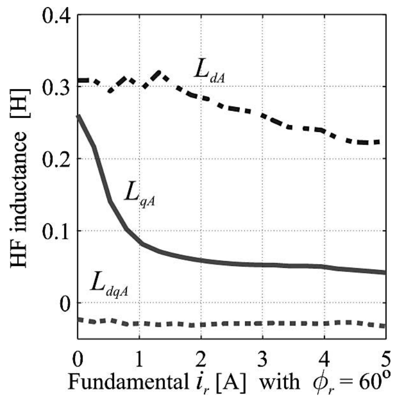

Fig. 5. RSM-anisotropy load dependence at standstill.

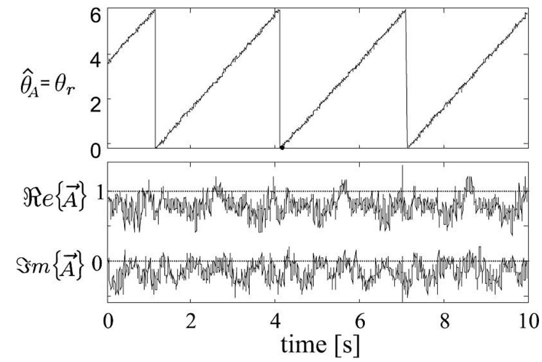

Fig. 6. RSM-anisotropy rotor-position-dependence at no load.

problems in the PLL due to the changing parameters. To maintain stability at all load conditions in this case, it was important to select the L_{dA} and L_{qA} parameters (for the normalization factor ΔL in the PLL) for the worst case scenario: that is when the difference between L_{qA} and L_{dA} is large, since the error signal then also becomes too large and causes instability. Therefore, the following constant parameters were chosen, i.e., $L_{dA} = 0.3$ H and $L_{qA} = 0.05$ H. Of course, the normalization factor ΔL can be varied online as a function of load (using an approximation function or a lookup table), but it has been found that this does not make a big difference to stability or dynamics compared to the case where the correct constant normalization factor is used.

The third test is to look at the dependency of the anisotropy on the actual rotor position. Up till now, all the tests have been done with a still standing rotor. It has been shown that the parameters L_{dA} and L_{qA} are dependent on the fundamental frequency current vector $\vec{i}_r$ and now it is the aim to see whether these parameters also depend on the rotor position θ_r. In this test, the estimated anisotropy angle is set equal to the actual rotor position $\hat{\theta}_A = \theta_r$; the HF voltage vector is applied as shown in Fig. 3 with $\delta = 0$; the fundamental frequency current is controlled to zero and the RSM is turned by another machine (the load machine, which is mechanically coupled to the RSM) at a low speed; the HF current amplitude $\vec{A}$ is calculated and normalized with the parameters L_{dA} and L_{qA} that correspond with zero fundamental current and the offset is subtracted from the real part of $\vec{A}$ so that the expected result is $\Re e\{\vec{A}\} = 1$ and $\Im m\{\vec{A}\} = 0$. In Fig. 6, it can seen that there is a change of $\vec{A}$ with rotor position, but it is not very large. In the ideal case, $\vec{A}$ must be constant, even with changing rotor position, since we set $\hat{\theta}_A = \theta_r$. But the fact that there is a small ripple indicates that the anisotropy is slightly rotor-position-dependent.

The fourth test is to close the PLL and check the closed-loop position estimation at all load conditions, at zero and low speed. For this test, the fundamental frequency current is controlled using the measured rotor position θ_r and the RSM is turned at a constant speed with the load machine. The HF voltage vector is applied in the direction of the estimated saliency position $\hat{\theta}_A$, with $\delta = 0$. If the normalization constant ΔL is correct, the PLL constants can be chosen as $K_p = 2BW$ and $K_i = BW^2$ to give a closed-loop bandwidth of BW and a damped response. A comparison between $\hat{\theta}_A$ and the measured θ_r for all load conditions is made, as in Fig. 7(a) for zero, half, and full load. It is found that the PLL prefers to track the q-axis of the RSM (this is the axis that is saturated most easily), but the anisotropy increasingly moves away from the q-axis as more and more load is applied. The arrows that point to each other in Fig. 7(a) show that the phase difference between the estimated anisotropy position and the actual rotor position changes from 99° for zero load, through 81° for half load to 69° for full load.

The rotor position can be estimated using the estimated saliency position $\hat{\theta}_A$, but a compensation function is necessary to add offset compensation (phase difference) $\theta_{\rm comp}$, as indicated in Fig. 3. In this case the compensation function could be approximated as a linear function: $\theta_{\rm comp} = \frac{-\pi}{180}(99 - 6 \cdot |\vec{i}_r^*|)$.

The final step is to use the estimated rotor position $\hat{\theta}_r = \hat{\theta}_A + \theta_{\rm comp}$ for the field-orientated control. Fig. 7(a) shows θ_r, $\hat{\theta}_r$, and $\hat{\theta}_A$ for low speed at loads of zero, half load, and rated load, while Fig. 7(b) shows the estimation error $\theta_r - \hat{\theta}_r$ that is made. It can be clearly seen that the rotor position estimation is very good at any load condition. Attention is drawn to the phase difference between $\hat{\theta}_A$ and θ_r in Fig. 7(a): with zero load, the phase difference is about 90°, i.e., the q-axis of the RSM is tracked, but as we increase the load, the phase difference becomes smaller, i.e., the saliency position moves towards the d-axis.

The rotor position estimation error that is made due to the position dependency of the anisotropy is not very significant in this RSM, and that is very good, because it is extremely difficult to compensate that kind of error. In can be noted, however, that under the no-load condition [see the top graph of Fig. 7(b)], the estimation error varies a lot with rotor position. The reason for this is that the q-axis of the RSM is no yet saturated under no load, and therefore, the inductance difference between L_{dA} and L_{qA} is small (as can be verified by Fig. 5). By applying only a little fundamental frequency q-axis current, the q-axis is saturated and the anisotropy position can be much better detected. Furthermore, the rotor position estimation error due to mutual inductance (offset error) can be successfully compensated, because it is a function of load current and can be approximated by a linear function, as shown in this case. It is critical to do

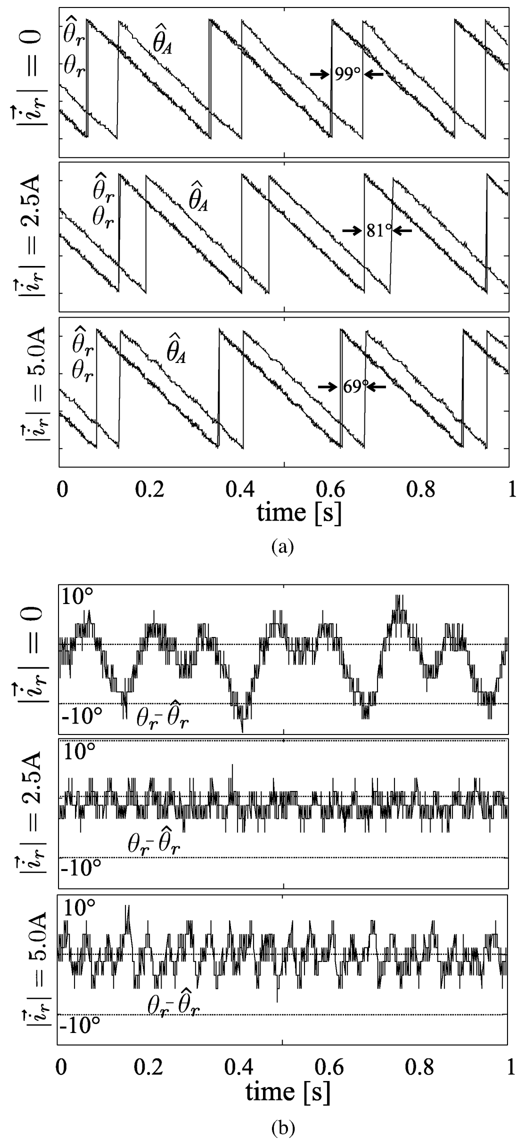

Fig. 7. RSM sensorless control at zero, half and rated load. (a) θ_r, $\hat{\theta}_e$ and $\hat{\theta}_A$ at low speed. (b) $\theta_r - \hat{\theta}_r$ at low speed.

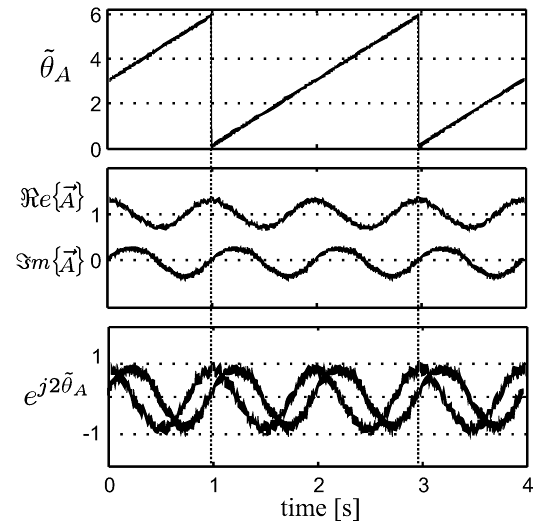

Fig. 8. PMSM-anisotropy at no load and standstill.

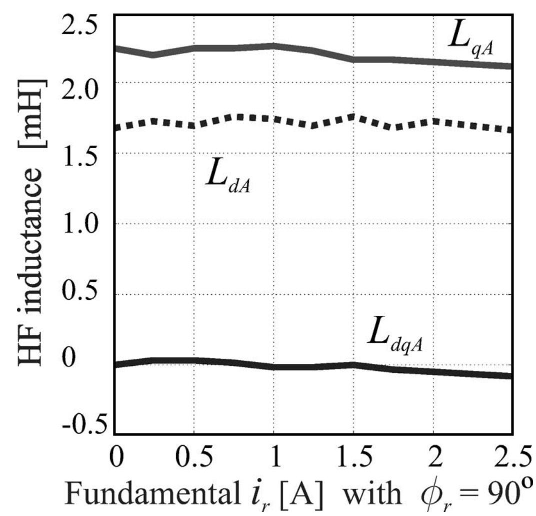

Fig. 9. PMSM-anisotropy load dependence at standstill.

this compensation to obtain the correct $\hat{\theta}_r$; otherwise, the wrong position will be used in field-oriented control, which will lead to loss in achieved torque, and possibly, instability.

V. PM Synchronous Machine

An off-the-shelf 0.5 kW PMSM, with a rated current of 1.6 A rms and a rated torque of 1.5 N·m, was also used to test the sensorless-field-orientated scheme for zero and low speed described in this paper and to compare it with the results for the RSM discussed previously. The first test is to find a suitable HF voltage: applying $U_{\rm HF} = 20\cos(2\pi 508)$ V results in a HF current $i_{\rm HF} = 0.2\sin(2\pi 508t + 0.4)$, i.e., 6% of the available voltage results in a HF current of 9% of the rated current. Therefore, $\zeta = 0.4\frac{180}{\pi} = 23°$, which represents about two samples delay with the sampling frequency of $f_s = 12\,205$ Hz, to align the demodulation sine wave $F_{\rm dem}$ with the HF current. It is noted that much less HF voltage is needed to achieve an HF current of about 10% of the rated current, as compared to the RSM. The acoustic noise due to the HF current is minimal.

In the second test, the parameters L_{dA} and L_{qA} for the no-load condition are determined (as explained earlier): $L_{dA} = 0.02$ H and $L_{dA} = 0.0255$ H. This measurement is shown in Fig. 8. It is noted that the inductance values are less than ten times in magnitude compared with the RSM's inductance values, and also that $L_{dA} < L_{qA}$, where, for the RSM, it is $L_{dA} > L_{qA}$. The dependency of L_{dA} and L_{qA} on the load current $\vec{i}_r$ (current angle of 90°) is tested and it is found that the parameters stay relatively constant for this PMSM, even up to rated current, as shown in Fig. 9. Up to this point, it seems like this machine would be easy to control sensorless and that the compensation function $\theta_{\rm comp}$ might not be necessary.

The third test is to look at the dependency of the anisotropy on the actual rotor position. As with the RSM, the following are done: set $\hat{\theta}_A = \theta_r$, inject the HF voltage with $\delta = 0$, and look at the normalized $\vec{A}$, where it is expected that $\Re e\{\vec{A}\} = 1$ and

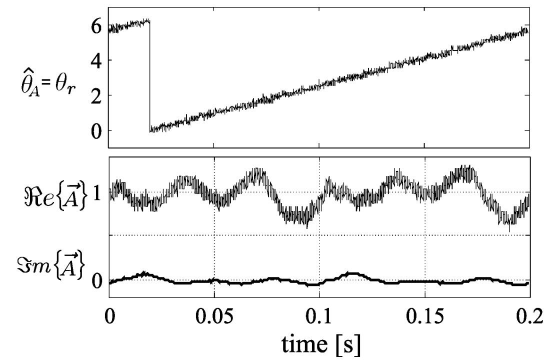

Fig. 10. PMSM-anisotropy rotor-position-dependence at no load.

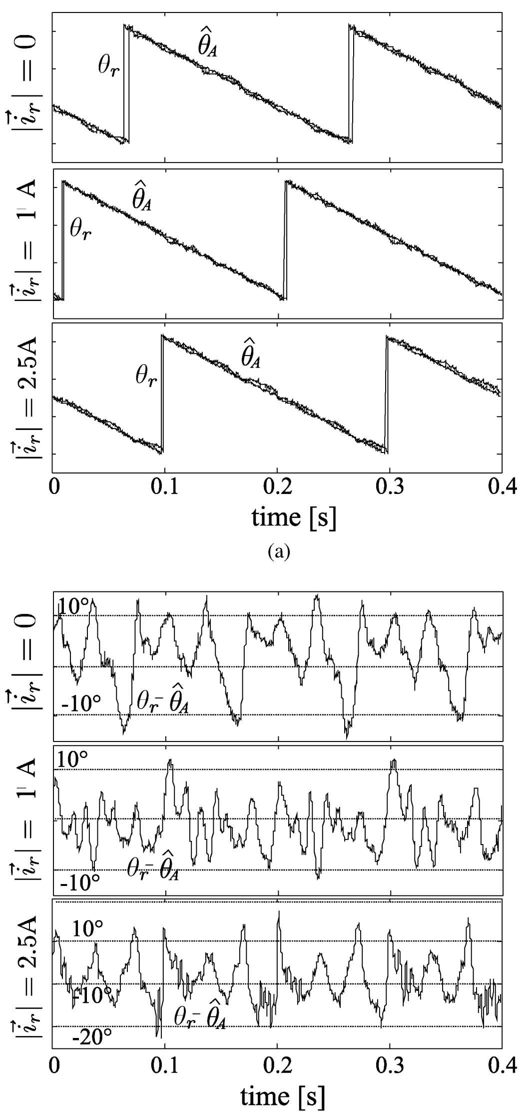

(a)

(b)

Fig. 11. θ comparison at zero, half, and rated load. (a) θ_r versus $\hat{\theta}_A$ at low speed. (b) $\theta_r - \hat{\theta}_A$ at low speed.

$\Im m\{\vec{A}\} = 0$. The result is shown in Fig. 10. The anisotropy for this PMSM has a stronger dependency on the rotor position, compared to the result of the RSM in Fig. 6. This test was also performed at half of the rated load and at rated load, and for each load condition, the position dependency looks different, although it is always periodic. Simulation was performed using the constant parameters for L_{dA} and L_{qA} to check if the fundamental current vector controller might be distorting the HF currents, but it was found that the problem is indeed a rotor-position-dependent anisotropy and not the current vector controller. Therefore, a rotor-position-varying estimation error is expected.

In the fourth test, the fundamental frequency current vector $\vec{i}_r$ is controlled using the measured position θ_r and the saliency position estimation is activated in parallel. The results for low speed with zero, half, and rated current are shown in Fig. 11(a), with the error between actual rotor position and estimated ansitropy position shown in Fig. 11(b). These results can be compared with the results for the RSM in Fig. 7(a) and (b).

For this PMSM, the saliency position seems to be aligned with the d-axis of the PMSM (where saturation caused by the PM causes a reduced inductance). At any given rotor position, the parameters L_{dA} and L_{qA} are not influenced so much by the fundamental current, i.e., they are more or less constant. However, the anisotropy is more dependent on the rotor position θ_r, i.e., for some rotor positions, the saliency position is equal to the rotor position, and for other rotor positions it is not. This kind of error is very difficult to compensate, since it is periodic in nature and also changes its shape for different loads.

VI. Conclusion

Position sensorless control of synchronous machines is an important and much researched theme, due to the cost reduction and reliability increase that it brings. A sensorless method has been identified to cope with zero- and low-speed requirements, and it involves the application of HF voltages and processing of HF currents that contain the saliency (anisotropy) position information. Under ideal circumstances, the saliency position is equal to the rotor position. However, the estimation algorithm that uses a simplified HF model with constant parameters is plagued by additional saturation caused by the fundamental frequency excitation. The estimation scheme is also disturbed by mutual inductance, which causes an offset error in the steady state. The offset error is load-dependent, but the problem can easily be solved by using a compensation function (as illustrated with a linearly approximated function in the case of the RSM, and see Fig. 3). The estimation scheme is further disturbed if the flux linkage in the dq reference frame is strongly rotor-position-dependent (dq flux linkage variation with rotor movement), which causes a rotor-position-varying component in the rotor position estimation error signal. This error is difficult to compensate and might lead to large estimation errors, as was shown for the PMSM. This paper has given more insight into the actual HF model (anisotropy model) of an RSM and PMSM, the effect that fundamental excitation and rotor position have upon it and how the results can be used to ensure stable sensorless control at zero and low speed.

REFERENCES

[1] M. Corley and R. Lorenz, "Rotor position and velocity estimation for a salient-pole permanent magnet synchronous machine at standstill and high speeds," *IEEE Trans. Ind. Appl.*, vol. 34, no. 4, pp. 784–789, Jul./Aug. 1998.

[2] M. Degner and R. Lorenz, "Using multiple saliencies for the estimation of flux, position, and velocity in ac machines," *IEEE Trans. Ind. Appl.*, vol. 34, no. 5, pp. 1097–1104, Sep./Oct. 1998.

[3] A. Consoli, G. Scarcella, and A. Testa, "Industry application of zero-speed sensorless control techniques for pm synchronous motors," *IEEE Trans. Ind. Appl.*, vol. 37, no. 2, pp. 513–521, Mar./Apr. 2001.

[4] M. Linke, R. Kennel, and J. Holtz, "Sensorless position control of permanent magnet synchronous machines without limitation at zero speed," in *Proc. IEEE 28th Annu. Conf. Ind. Electron. Soc. (IECON 2002)*, R. Kennel, Ed., vol. 1, pp. 674–679.

[5] S. Morimoto, K. Kawamoto, M. Sanada, and Y. Takeda, "Sensorless control strategy for salient-pole pmsm based on extended emf in rotating reference frame," *IEEE Trans. Ind. Appl.*, vol. 38, no. 4, pp. 1054–1061, Jul./Aug. 2002.

[6] J. Faiz and S. Mohseni-Zonoozi, "A novel technique for estimation and control of stator flux of a salient-pole pmsm in dtc method based on mtpf," *IEEE Trans. Ind. Electron.*, vol. 50, no. 2, pp. 262–271, Apr. 2003.

[7] H. Kim, M. Harke, and R. Lorenz, "Sensorless control of interior permanent-magnet machine drives with zero-phase lag position estimation," *IEEE Trans. Ind. Appl.*, vol. 39, no. 6, pp. 1726–1733, Nov./Dec. 2003.

[8] M. Linke, R. Kennel, and J. Holtz, "Sensorless speed and position control of synchronous machines using alternating carrier injection," in *Proc. IEEE Int. Electr. Mach. Drives Conf. (IEMDC 2003)*, vol. 2, pp. 1211–1217.

[9] M. Haque, L. Zhong, and M. Rahman, "A sensorless initial rotor position estimation scheme for a direct torque controlled interior permanent magnet synchronous motor drive," *IEEE Trans. Power Electron.*, vol. 18, no. 6, pp. 1376–1383, Nov. 2003.

[10] H. Kim, K.-K. Huh, R. Lorenz, and T. Jahns, "A novel method for initial rotor position estimation for ipm synchronous machine drives," *IEEE Trans. Ind. Appl.*, vol. 40, no. 5, pp. 1369–1378, Sep./Oct. 2004.

[11] Y.-s. Jeong, R. Lorenz, T. Jahns, and S.-K. Sul, "Initial rotor position estimation of an interior permanent-magnet synchronous machine using carrier-frequency injection methods," *IEEE Trans. Ind. Appl.*, vol. 41, no. 1, pp. 38–45, Jan./Feb. 2005.

[12] O. Wallmark, L. Harnefors, and O. Carlson, "An improved speed and position estimator for salient permanent-magnet synchronous motors," *IEEE Trans. Ind. Electron.*, vol. 52, no. 1, pp. 255–262, Feb. 2005.

[13] P. Acarnley and J. Watson, "Review of position-sensorless operation of brushless permanent-magnet machines," *IEEE Trans. Ind. Electron.*, vol. 53, no. 2, pp. 352–362, Apr. 2006.

[14] N. Imai, S. Morimoto, M. Sanada, and Y. Takeda, "Influence of magnetic saturation on sensorless control for interior permanent-magnet synchronous motors with concentrated windings," *IEEE Trans. Ind. Appl.*, vol. 42, no. 5, pp. 1193–1200, Sep./Oct. 2006.

[15] S. Morimoto, M. Sanada, and Y. Takeda, "Mechanical sensorless drives of IPMSM with online parameter identification," *IEEE Trans. Ind. Appl.*, vol. 42, no. 5, pp. 1241–1248, Sep./Oct. 2006.

[16] C. Silva, G. Asher, and M. Sumner, "Hybrid rotor position observer for wide speed-range sensorless pm motor drives including zero speed," *IEEE Trans. Ind. Electron.*, vol. 53, no. 2, pp. 373–378, Apr. 2006.

[17] J. Hu, L. Xu, and J. Liu, "Eddy current effects on rotor position estimation for sensorless control of pm synchronous machine," in *Proc. 41st IAS Annu. Meet., Conf. Rec. IEEE Ind. Appl. Conf.*, 2006, L. Xu, Ed., vol. 4, pp. 2034–2039.

[18] N. Bianchi and S. Bolognani, "Influence of rotor geometry of an ipm motor on sensorless control feasibility," *IEEE Trans. Ind. Appl.*, vol. 43, no. 1, pp. 87–96, Jan./Feb. 2007.

[19] N. Bianchi, S. Bolognani, J.-H. Jang, and S.-K. Sul, "Comparison of pm motor structures and sensorless control techniques for zero-speed rotor position detection," *IEEE Trans. Power Electron.*, vol. 22, no. 6, pp. 2466–2475, Nov. 2007.

[20] H. Hida, Y. Tomigashi, and K. Kishimoto, "Novel sensorless control for pm synchronous motors based on maximum torque control frame," in *Proc. Eur. Conf. Power Electron. Appl.*, Y. Tomigashi, Ed., 2007, pp. 1–10.

[21] S. Taniguchi, S. Wakao, K. Kondo, and T. Yoneyama, "Position sensorless control of permanent magnet synchronous motor at low speed range using harmonic voltage injection," in *Proc. Eur. Conf. Power Electron. Appl.*, S. Wakao, Ed., 2007, pp. 1–7.

[22] D. Raca, P. Garcia, D. Reigosa, F. Briz, and R. Lorenz, "A comparative analysis of pulsating vs. rotating vector carrier signal injection-based sensorless control," in *Proc. 23rd Annu. IEEE Appl. Power Electron. Conf. Expo. (APEC 2008)*, P. Garcia, Ed., pp. 879–885.

[23] M. Arefeen, M. Ehsani, and A. Lipo, "Sensorless position measurement in synchronous reluctance motor," *IEEE Trans. Power Electron.*, vol. 9, no. 6, pp. 624–630, Nov. 1994.

[24] R. Lagerquist, I. Boldea, and T. Miller, "Sensorless-control of the synchronous reluctance motor," *IEEE Trans. Ind. Appl.*, vol. 30, no. 3, pp. 673–682, May/Jun. 1994.

[25] M. Schroedl and P. Weinmeier, "Sensorless control of reluctance machines at arbitrary operating conditions including standstill," *IEEE Trans. Power Electron.*, vol. 9, no. 2, pp. 225–231, Mar. 1994.

[26] P. Jansen and R. Lorenz, "Transducerless position and velocity estimation in induction and salient ac machines," *IEEE Trans. Ind. Appl.*, vol. 31, no. 2, pp. 240–247, Mar./Apr. 1995.

[27] T. Matsuo and T. Lipo, "Rotor position detection scheme for synchronous reluctance motor based on current measurements," *IEEE Trans. Ind. Appl.*, vol. 31, no. 4, pp. 860–868, Jul./Aug. 1995.

[28] P. Jansen and R. Lorenz, "Transducerless field orientation concepts employing saturation-induced saliencies in induction machines," *IEEE Trans. Ind. Appl.*, vol. 32, no. 6, pp. 1380–1393, Nov./Dec. 1996.

[29] M. Jovanovic, R. Betz, and D. Platt, "Sensorless vector controller for a synchronous reluctance motor," *IEEE Trans. Ind. Appl.*, vol. 34, no. 2, pp. 346–354, Mar./Apr. 1998.

[30] A. Consoli, F. Russo, G. Scarcella, and A. Testa, "Low- and zero-speed sensorless control of synchronous reluctance motors," *IEEE Trans. Ind. Appl.*, vol. 35, no. 5, pp. 1050–1057, Sep./Oct. 1999.

[31] S.-J. Kang, J.-M. Kim, and S.-K. Sul, "Position sensorless control of synchronous reluctance motor using high frequency current injection," *IEEE Trans. Energy Convers.*, vol. 14, no. 4, pp. 1271–1275, Dec. 1999.

[32] M.-T. Lin and T.-H. Liu, "Sensorless synchronous reluctance drive with standstill starting," *IEEE Trans. Aerosp. Electron. Syst.*, vol. 36, no. 4, pp. 1232–1241, Oct. 2000.

[33] A. Vagati, M. Pastorelli, F. Scapino, and G. Franceschini, "Impact of cross saturation in synchronous reluctance motors of the transverse-laminated type," *IEEE Trans. Ind. Appl.*, vol. 36, no. 4, pp. 1039–1046, Jul./Aug. 2000.

[34] E. Capecchi, P. Gugliehni, M. Pastorelli, and A. Vagati, "Position-sensorless control of the transverse-laminated synchronous reluctance motor," *IEEE Trans. Ind. Appl.*, vol. 37, no. 6, pp. 1768–1776, Nov./Dec. 2001.

[35] T. Senjyu, T. Shingaki, and K. Uezato, "Sensorless vector control of synchronous reluctance motors with disturbance torque observer," *IEEE Trans. Ind. Electron.*, vol. 48, no. 2, pp. 402–407, Apr. 2001.

[36] C.-G. Chen, T.-H. Liu, M.-T. Lin, and C.-A. Tai, "Position control of a sensorless synchronous reluctance motor," *IEEE Trans. Ind. Electron.*, vol. 51, no. 1, pp. 15–25, Feb. 2004.

[37] P. Guglielmi, M. Pastorelli, G. Pellegrino, and A. Vagati, "Position-sensorless control of permanent-magnet-assisted synchronous reluctance motor," *IEEE Trans. Ind. Appl.*, vol. 40, no. 2, pp. 615–622, Mar./Apr. 2004.

[38] P. Guglielmi, M. Pastorelli, and A. Vagati, "Impact of cross-saturation in sensorless control of transverse-laminated synchronous reluctance motors," *IEEE Trans. Ind. Electron.*, vol. 53, no. 2, pp. 429–439, Apr. 2006.

[39] S. Ichikawa, M. Tomita, S. Doki, and S. Okuma, "Sensorless control of synchronous reluctance motors based on extended emf models considering magnetic saturation with online parameter identification," *IEEE Trans. Ind. Appl.*, vol. 42, no. 5, pp. 1264–1274, Oct. 2006.

[40] A. Consoli, G. Scarcella, G. Scelba, A. Testa, and D. Triolo, "Sensorless rotor position estimation in synchronous reluctance motors exploiting a flux deviation approach," *IEEE Trans. Ind. Appl.*, vol. 43, no. 5, pp. 1266–1273, Sep./Oct. 2007.

[41] H. de Kock, M. Kamper, O. Ferreira, and R. Kennel, "Position sensorless control of the reluctance synchronous machine considering high frequency inductances," in *Proc. Power Electron. Drive Syst. (PEDS 2007)*, pp. 812–821.

[42] A. J. Rix, M. J. Kamper, and R.-J. Wang, "Design and performance evaluation of concentrated coil permanent magnet machines for in-wheel drives," in *Proc. IEEE Int. Electr. Mach. Drives Conf. (IEMDC 2007)*, M. J. Kamper, Ed., vol. 1, pp. 770–775.
[43] F. Magnussen and H. Lendenmann, "Parasitic effects in pm machines with concentrated windings," in *2005 IEEE Ind. Appl. Conf.*, vol. 43, no. 5, pp. 1223–1232, Sep./Oct. 2007.
[44] O. Wallmark and L. Harnefors, "Sensorless control of salient pmsm drives in the transition region," *IEEE Trans. Ind. Electron.*, vol. 53, no. 4, pp. 1179–1187, Jun. 2006.

Hugo W. De Kock (M'06) received the B.Eng. and M.Sc.Eng (with honours) degrees in 2006 from Stellenbosch University, Matieland, South Africa., where he also received the Ph.D. Eng. degree in 2009. His Ph.D. study focused on position sensorless and optimal torque control of synchronous machines. He spent two years at the University of Wuppertal in Germany as part of his Ph.D. study and was a DAAD scholarship holder.

He is currently a Development Engineer in the automotive industry. His current research interests include the application of electrical drives in electrical vehicles.

Maarten J. Kamper (M'96–SM'08) received the M.Sc. (Eng.) and Ph.D. degrees in 1987 and 1996, respectively, both from the University of Stellenbosch, Stellenbosch, South Africa.

He has been on the academic staff of the Department of Electrical and Electronic Engineering, University of Stellenbosch, since 1989, and is currently a Professor of electrical machines and drives. His research interests include computer-aided design and control of reluctance, permanent magnet and induction machine drives.

Prof. Kamper is a South African National Research Foundation-Supported Scientist and a Registered Professional Engineer in South Africa.

Ralph M. Kennel (M'89–SM'96) reeived the Dr.-Ing. (Ph.D.) degree from the University of Kaiserslautern in 1984.

From 1983 to 1999, he was holding several positions with Robert BOSCH GmbH, Germany. Until 1997, he was engaged in the development of servo drives. Between 1997 and 1999, he was responsible for "Advanced and Product Development of Fractional Horsepower Motors" in automotive applications. From 1994 to 1999, he was appointed Visiting Professor at the University of Newcastle-upon-Tyne, U.K. Since 1999, he has been a Professor for electrical machines and drives at Wuppertal University, Germany. Since 2008, he is a Professor for electrical drive systems and power electronics at the Technische Universität München, München, Germany. His current research interests include sensorless control of ac drives, predictive control of power electronics, and hardware-in-the-loop systems.

Prof. Kennel is a Fellow of Institution of Electrical Engineers, U.K., and a Chartered Engineer in the U.K.

IEEE POWER ELECTRONICS SOCIETY

Digital Object Identifier 10.1109/TPEL.2009.2029999

INFORMATION FOR AUTHORS

The IEEE TRANSACTIONS ON POWER ELECTRONICS is published bimonthly in January, March, May, July, September and November. Its scope includes new results in the field of power electronics. For example, papers that treat original component, device, module, circuit, control, system, or application issues are of interest. Papers that do not show sufficient overlap with interest in the power electronics field (a few examples are device physics, component manufacturing technologies, and circuit theory) should be submitted to other IEEE TRANSACTIONS that cover these fields. Authors should pay particular attention to documenting their work in relationship to the known literature. Papers of a historical or tutorial nature within the scope of this publication will also be considered.

Manuscript types: Three types of manuscripts are accepted.

- **Regular papers:** Typically eight pages in final length.
- **Letters:** Four or fewer pages in final form, intended for rapid processing. Typical contributions should focus on a specific, original contribution, with sufficient literature review, analysis, and results to establish clearly its merit and potential value. Clarity is especially important in short papers. Contributions likely to stimulate additional ideas or unusual lines of thought for electronic power conversion are of special interest. Rapid publication is achieved for Letter Papers by means of efficient review and reduced cycles of revision.
- **Correspondence:** These normally address corrections to published papers or substantive technical discussion of papers. They are limited to two pages in final form.

Papers submitted for consideration should report on original results not previously presented in any other archival publication, including but not limited to any IEEE TRANSACTIONS. Notwithstanding this requirement, papers previously presented and published in a Conference Record or Conference Proceedings, such as the IEEE Power Electronics Specialists Conference (PESC), Applied Power Electronics Conference (APEC), International Telecommunications Energy Conference (INTELEC), and the like will be considered although it is not required for a paper to have been presented or published at a conference to make it eligible for consideration by the IEEE TRANSACTIONS ON POWER ELECTRONICS. Copyright release may be required if the conference publication is copyrighted by an entity other than the IEEE. Authors must indicate in their submission any prior presentation and publication at a conference or prior submission to any other publication. It is the responsibility of the authors to obtain a copyright release if required for submission to the TRANSACTIONS. It is furthermore the responsibility of authors to ensure that papers submitted for review are formulated in acceptable English. Inadequate English obscures the technical content of the manuscript and will be grounds for rejection.

Guidelines for Submitting a Paper for Review

These Guidelines are specified by the PELS Editor in Chief.

The IEEE Power Electronics Society employs *Manuscript Central,* a professional web-based manuscript submission and peer-review tracking system. Authors ***must submit manuscripts electronically*** (as .pdf or .ps files) to http://mc.manuscriptcentral.com/tpel-ieee. From this entry page, access can be obtained to all information required for the submission of a manuscript. Please note that **first-time users must create a new account.** All authors are responsible for understanding these guidelines before submitting a manuscript for consideration. A help system is available on the web site, including telephone contacts.

Papers in the two-column single-spaced format common for conference publication are not acceptable, as this form is difficult for reviewers. The paper should be prepared based on one side of letter-size paper (either $8.5'' \times 11''$ or A4 sizes), and should be in single-column double-spaced format. The paper should include all figures, tables, captions, and references. Author biographies, photos, and copyright form are not required for the initial submission. Please use standard fonts such as Times Roman (serif), Helvetica (sans serif), and Symbol. Unusual fonts may create incompatibilities that delay processing. It is the authors' responsibility to make sure the submitted files (in PDF or .ps format) are fully viewable and in the intended format.

The first page should contain the paper title, full first and last names of all authors (do not use an initial for the first name), and author organizational affiliation. Paper titles should avoid extraneous words such as "new" or "novel" that have limited search value. The corresponding author must be indicated clearly, along with the corresponding author's title, name, postal address, voice telephone number, fax telephone number, and e-mail address. The first page should also indicate whether or not the paper has been presented at a conference or submitted elsewhere previously, and if so should specify the conference name, dates, and location. The first page should also contain an abstract of not more than 200 words. The abstract should not only indicate the subject and scope of the paper but should also summarize, if possible, the author's conclusion, so that the abstract itself may be a useful document in an information-retrieval system. The authors should provide a list of up to five keywords for indexing purposes. Begin the main text of the paper on the second page.

Papers submitted to the PELS Editor are to be of original content and void of significant duplication with other papers by the same or different authors. In addition, by submitting to PELS the author is acknowledging that the paper has not been submitted to any other journal simultaneously, with the exception being conference papers as described under the "Information for Authors" section.

For readability in the review process, figures and tables may be interspersed in the text of the submitted manuscript and be accompanied by captions. Alternatively the authors may choose to use separate figures, tables, and captions as specified by the instructions for the final paper as shown below. Authors should avoid using color in the manuscript unless the resulting graphics are fully legible and clear in monochrome reproduction. The final manuscript can include color content only if the authors intend to use and pay for color pages in the final paper as required by IEEE.

An effective literature review is essential to any submission. Inadequate references are grounds for rejection. References should be indicated using numbers in square brackets (e.g. [1], [2], and [3]), should be in a separate section at the end of the paper, and should be in IEEE style:

- **Style for conference publications:** Authors (first initials followed by last name), title of paper, in title of conference, dates of conference, location of conference, and page numbers (inclusive). Example: A. B. Researcher and I. N. Elper, "Loss-based analysis of switching converters under closed-loop controls," in *Proc. IEEE Applied Power Electronics Conf.,* 2010, pp. 3917-3926.
- **Style for periodical journal publications:** Authors (first initials followed by last name), title of paper, title of periodical, volume, page numbers (inclusive), month, and year. Example: C. D. Aodiet, R. G. Gue, and P. R. Phakter, "The Ran-Duga method for ac-ac converter operation," *IEEE Trans. Power Electronics,* vol. 37, pp. 7721-7727, October 2014.
- **Style for books:** Authors (first initials followed by last name), book title. Publisher location: publisher name, year, chapter or page numbers. Example: B. B. Eriffel, *The Design of Microwatt Power Devices.* London: Energy Unit Publishers, 2012, Chap. 72.

Authors should attempt to limit paper length so that, should it be accepted for publication in the TRANSACTIONS, the final result is eight pages or fewer in length for regular papers and three pages or fewer for letter papers. Longer papers are subject to mandatory overlength page charges, as discussed below. The submission of papers in a series (Part I, Part II, etc.) on the same subject is normally discouraged as a matter of policy. In such cases the authors may be asked to consolidate the work into a single submission.

Mandatory overlength page charges for Regular papers will apply to page nine and above and mandatory overlength page charges for Letters will apply to page five and above. For 2006, the overlength page charge is US$162/page. Authors must agree to pay the page charges in advance of publication. When submitting the paper for review, estimate the length of a paper using the following method:

- Three (3) pages of text in single-column double-spaced format translate to approximately one page when published in the TRANSACTIONS.
- Six (6) figures translate to approximately one page when published in the TRANSACTIONS For the purposes of estimation, count as separate figures different parts of the same figure. For example, if Figure 1 has parts (a), (b), and (c), then for the purposes of estimating final paper length Figure 1 is estimated to take approximately one half of a published TRANSACTIONS page.

This method is only an approximation and the authors are responsible for page charges regardless of any previously estimated length of the paper.

Digital Object Identifier 10.1109/TPEL.2009.2030001

Letters Submissions

Papers indicated by authors as "Letters" submissions are considered through an expedited review process by a special team of associate editors. The objective is to provide the quickest possible route to publication for short, focused papers on topics of current interest. The process is accelerated because only short manuscripts are considered and because a publication decision is made after the first set of reviews become available. Authors who wish to have a publication considered this way should limit the manuscript to nine double-spaced pages in addition to the title page described above. Please indicate on the title page that the paper is to be considered for Letters. The Power Electronics Society continues to actively support and encourage submissions of this type as a way to reduce publication time.

Checklist and Guidelines for Submitting a Final Paper for Publication

Information provided below is current as of 1 January 2007. Only after notification of acceptance will these materials be required.

Guidelines for Submitting a Final Paper for Publication

After a paper has been accepted for publication the authors will be notified by the PELS Editor. When corrections for format and other information are completed, the original single-column, double-space electronic version of the paper (Font: Times New Roman preferred, size no less than 10 point, no larger than 12 point) along with electronic files for the illustrations, will be forwarded to IEEE for final formatting. Authors should not prepare camera-ready copy. The final paper for publication should include a complete mailing address for every author and should indicate whether each author is an IEEE member.

The text of the paper will be typeset by the IEEE. In contrast, figures and tables will be produced directly from the versions submitted by the authors. For the final submission, figures and tables should not be embedded in the text but should be on separate pages in single-column format with, preferably, one figure per page. Originals for figures should be of the highest quality: sharp, noise free, and of good contrast. Line drawings should be in black on a white background suitable for printing on a high-quality laser printer. Figures consisting of photographs must be glossy prints or should be provided in tiff or jpeg. Figures should be no larger than 8×10 in (20.3×25.4 cm). Use lettering on figures only where necessary. All lettering on figures must be of uniform size and large enough to permit legible reduction to column width (3.5 in or 8.9 cm). If the final version is intended to use color figures, there will be an extra basic charge of $1,045.00 (depending on the number of figures) plus an additional $125.00 for each color figure. If the final version is not intended to be in color, the authors must assure that gray scale versions of any color content will be clear and legible.

Electronic submission of the final paper is required. The following general requirements should be observed:

- Submit the text of the paper in the native electronic format of the word processing software used to create it. The final manuscript will be re-converted from the original, not from the review .pdf copy. The operating system and word processing software used to produce the paper should be noted (e.g., Windows/Microsoft Word). The formats with best support are Microsoft Word (versions 95 and later) and LaTex. If a compressed or segmented file is sent, be sure to indicate the method of compression (e.g., ".zip," ".sit"). Please do not include extraneous files.
  ◦ The electronic copy should be checked by the authors for consistency with the expected printed format.
- Include a flat ASCII version (text only) with the word-processed version. This helps facilitate the conversion process. A .pdf version which exactly matches the intended final version should be included to check for any difficulties in illustrations or fonts.
- Figures and tables are also submitted electronically. Each figure and table is to be in its own file without caption and labeled fig1, fig2 (lower case without further identification). For figures and tables with multiple parts: figure parts that should appear side by side should be in the same file, without caption. Figure parts that should appear above or below should be in separate files, without caption. Full and complete figure and table captions should be provided in a separate file. A text-only version of any tables should be sent as well, without table lines.
- Files containing a brief biography and a digital version of a personal photo (passport type at a resolution of not less than 300 pixels per inch) of each author should be included for Regular papers but not for Letters or Correspondence.
- All the files above should be compressed in (e.g., ".zip," ".sit," "stuffit") and sent by email to:

Dr. Frede Blaabjerg, *Editor in Chief*
Aalborg University,
Institute of Energy Technology
Pontoppidanstraede 101
Dk-9220 Aalborg East, Denmark peleditor@ieee.org

Page Charges

Regular papers published in the PELS TRANSACTIONS should normally be eight or fewer pages. Letter papers should plan for three pages or fewer. For regular papers, pages nine and above will incur an excess page charge of $162 per page. For letter papers, pages five and above will incur this page charge. After the final paper has been submitted, the PELS Editor will estimate the length of the final paper using the formula given above, and will notify the author of the potential for excess page charges. Authors must commit to paying excess page charges before the paper is sent to the IEEE for publication.

After production of the final paper by IEEE and prior to final publication, the IEEE will send "galley proofs" to the author for final editing. Page charges will be assessed at this time.

Copyright

It is the policy of the IEEE to own the copyright to the technical contributions it publishes on behalf of the interests of the IEEE, its authors, and their employers, and to facilitate the appropriate reuse of this material by others. To comply with the U.S. Copyright Law, authors are required to sign an IEEE copyright form before publication. This form returns to authors and their employers full rights to reuse their materials for the their own purposes. Authors should submit a signed copy of this form with their papers.

Additional Information: **IEEE Guide for Transactions Authors**

Digital Object Identifier 10.1109/TPEL.2009.2030000